

1 **Singing comet waves in a solar wind convective electric**  
2 **field frame**

3 **C. Goetz<sup>1</sup>, F. Plaschke<sup>2</sup>, and M. G. G. T Taylor<sup>1</sup>**

4 <sup>1</sup>ESTEC, European Space Agency, Noordwijk, The Netherlands.  
5 <sup>2</sup>Space Research Institute, Austrian Academy of Sciences, Graz, Austria.  
6 <sup>1</sup>Keplerlaan 1, 2201AZ Noordwijk, The Netherlands.  
7 <sup>2</sup>Schmiedlstrasse 6, 8042 Graz, Austria.

8 **Key Points:**

- 9 • Low-frequency waves may be found everywhere in the coma, regardless of the con-  
10 vective electric field direction.  
11 • The wave frequency decreases with decreasing heliocentric distance.  
12 • There is no correlation of the plasma density with the wave frequency.

**Abstract**

The cometary plasma environment at low gas production rates is dominated by highly compressional, large amplitude magnetic field waves in the 10–100 mHz range. They are thought to be caused by an ion-Weibel instability due to a cross-field current, which is caused by the cometary ions that are accelerated along the solar wind convective electric field. We devise a new method to determine the location of the wave detection, the wave power, frequency, and bandwidth. It is found that the wave occurs everywhere in the coma, regardless of electric field direction. There is no correlation between the wave frequency and the measured plasma density. This is not in agreement with previous studies. A dependence of the frequency on the position of the spacecraft in a comet-fixed frame is in agreement with the prediction from the ion-Weibel instability. We infer a wave generation region much larger than the distances covered by Rosetta.

**Plain Language Summary**

We study the properties and region of occurrence of so-called singing comet waves. This type of electromagnetic wave has only been observed at comet 67P/Churyumov-Gerasimenko at low gas production rates. Contrary to previous publications our results indicate that this wave is not only found in one hemisphere of the comet’s plasma environment. Instead it is generated in a much bigger region around the nucleus than previously known.

**1 Introduction**

Comets are small solar system bodies composed of ices and rock. As comets approach the Sun, the ices sublime and form a neutral gas coma around the nucleus that is not gravitationally bound. The gas is ionized mainly by photo-ionization and electron impact ionization. The resulting ion cloud presents an obstacle to the solar wind, as the newly formed ions are at rest in the cometary frame of reference. To incorporate the cometary ions into the solar wind they need to be accelerated which may be accomplished by an  $E \times B$  drift that is associated with the convective electric field of the solar wind (Behar et al., 2016). As the cometary ions are mainly water and the solar wind magnetic field magnitude is low, the gyroradius of the cometary ions can exceed 10000 km under low outgassing conditions at high heliocentric distances (Glassmeier, 2017).

The Jupiter family comet 67P/Churyumov-Gerasimenko was explored by the European Space Agency’s Rosetta mission for an entire perihelion passage from 2014 to 2016 (Glassmeier, Boehnhardt, et al., 2007). The spacecraft was equipped with a full suite of plasma instruments that explored the interaction of the solar wind with the cometary charged particle environment.

Since its arrival at the comet, Rosetta has measured various plasma waves, most notably a new type of low frequency wave in the vicinity of a weakly outgassing comet was found by Richter et al. (2015). They show that large amplitude, compressional waves are detected around frequencies of 40 mHz. The wave frequency does not depend on the background magnetic field. This type of wave is new compared to observations at other comets, where a wave in the frequency range of the ion-cyclotron frequency (which depends on the magnetic field magnitude) was detected. Richter et al. (2015) find that the “wave activity in general is controlled by the cometary ion production rate” and that the magnetic energy density in the 30–80 mHz band increases with decreasing cometocentric distance down to a distance of about 30 km. The proposed generation mechanism for this wave activity is a cross-field current. This mechanism is further investigated theoretically by Meier et al. (2016), who find a zero frequency wave that is subject to a Doppler shift to the spacecraft frame of reference.

61 Richter et al. (2016) and Heinisch et al. (2017) study the properties of these waves  
 62 using both Rosetta and the lander Philae’s observation of the magnetic field. They find  
 63 that both spacecraft measure the same wave phenomena, indicating that the generation  
 64 region is larger than the separation ( $\sim 10$  km) of the two spacecraft. They infer a wave-  
 65 length of tens to hundreds of km and show that the wave signature is broadband and  
 66 variable between  $\sim 10$  mHz and  $\sim 100$  mHz. They report an upper size limit for the  
 67 generation region of 100 km.

68 Simulations of the plasma environment of a weakly outgassing comet reveal struc-  
 69 tures that can be interpreted as waves (Koenders et al., 2016). They are exclusively found  
 70 in the  $+E$  hemisphere of the interaction region, where  $E$  is the solar wind convective elec-  
 71 tric field. A second simulation reveals that even at higher gas production rates, the waves  
 72 are present and confined to one hemisphere.

73 Hajra et al. (2017) investigate the plasma’s reaction to a cometary outburst (Grün  
 74 et al., 2016). It is found that the singing comet waves vanish around the time of the high-  
 75 est plasma density. In a follow-up study by Breuillard et al. (2019) this is investigated  
 76 further with one of the main results being that the waves do not vanish, instead the fre-  
 77 quency is lowered (from  $\sim 50$  mHz to  $\sim 20$  mHz). They conclude that this decrease is  
 78 due to the additional ion-neutral friction slowing down the cometary ions and thus chang-  
 79 ing the Doppler shift of the wave frequency.

80 It is also found that the singing comet power is diminished in one hemisphere of  
 81 the coma in the near-tail (Volwerk et al., 2018). It is speculated that this is due to the  
 82 orientation of the convective electric field, which should influence the location of the gen-  
 83 eration region of the waves.

84 In this publication we investigate for the first time where these low-frequency waves  
 85 are detected in the plasma environment especially with regards to the convective elec-  
 86 tric field direction and how their frequency evolved with time during the pre-perihelion  
 87 time period of the Rosetta mission.

## 88 2 Data and Methods

89 We use magnetic field measurements from the Rosetta Plasma Consortium (RPC)  
 90 magnetometer (MAG) (Glassmeier, Richter, et al., 2007), resampled to 1 Hz in cometo-  
 91 centric solar equatorial (CSEQ) coordinates. When burst mode data is available, we use  
 92 a filter with a cutoff frequency of 0.9 Hz to resample to 1 Hz (to ensure suppression of  
 93 all high frequency contributions), in normal mode the onboard filter is used. We use data  
 94 from August 2014 to end of March 2015. This interval was chosen to cover as many gas  
 95 production rates and cometocentric distances as possible, while retaining the best avail-  
 96 able data quality. The end of March cutoff was chosen because it is roughly where the  
 97 solar wind ion cavity is larger than the spacecraft cometocentric distance and Rosetta  
 98 is considered to be orbiting in the inner coma. This corresponds to a gas production rate  
 99 of roughly  $5 \times 10^{26} \text{ s}^{-1}$ . Only one interval has a suitable orbit to investigate the behaviour  
 100 of the waves at similar gas production rates and far from the nucleus: the tail excursion  
 101 in March 2016 (Volwerk et al., 2018). This interval is not included in the statistical study  
 102 because the magnetic field is not as reliable due to a lack of calibration opportunities.  
 103 With a more cautious approach to the magnetic field measurements, it can still be used  
 104 for a case study, as was done in Volwerk et al. (2018).

105 We develop a new method to detect wave activity and the wave properties. We com-  
 106 pute the power spectral density in a 600 s sliding interval with an overlap of 300 s. For  
 107 the power spectral density estimator we use Welch’s method with an interval length of  
 108 0.25 of the original signal length and an overlap of 0.125. From this the 95 % confidence  
 109 interval is computed as well. Then a linear fit (in a double logarithmic plot) is made for  
 110 all frequencies below 0.1 mHz. This cutoff frequency was chosen due to the filter cutoff

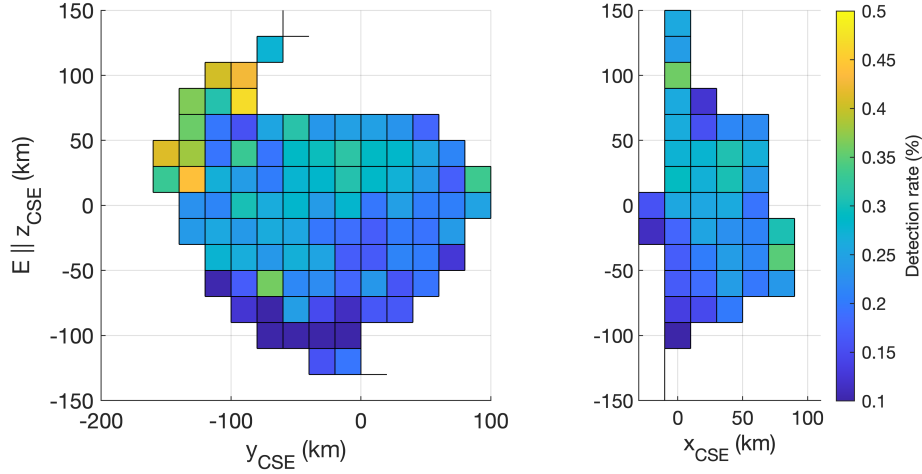


**Figure 1.** Distribution of the wave detections in two planes of the CSE frame. The spacecraft coverage for the same planes is shown in Fig. 2.

111 that is used to resample the magnetometer data onboard (normal mode). This filter cut-  
 112 off makes it very difficult to correctly interpret frequencies above  $\sim 200$  mHz. Then the  
 113 spectrogram is detrended using the linear fit and the largest peak is determined. A pos-  
 114 itive wave detection is logged if the peak prominence is more than two times the con-  
 115 fidence interval.

116 Richter et al. (2016) uses a different method to determine the properties of the singing  
 117 comet waves. This method involves computing the PSD estimate in a sliding interval and  
 118 then integrating in a spectral band between 10 mHz and 100 mHz. However, this method  
 119 does not distinguish intervals that have a clear wave signature from intervals without  
 120 one.

121 We use the reference frame CSE (cometocentric solar electric), in which the x-axis  
 122 points toward the Sun, the z-axis points along the convective electric field, and y com-  
 123 pletes the right handed system. Since Rosetta has no instrument to determine the con-  
 124 vective electric field, we estimate its direction by  $\vec{E} = -\vec{v} \times \vec{B}$ , whereby  $\vec{B}$  is the mea-  
 125 sured field. The solar wind velocity  $\vec{v}$  is estimated to be 400 km/s pointing in anti-sunward  
 126 direction. This is similar to the approach taken by Edberg et al. (2019). Since it is only  
 127 the direction of the solar wind that is of importance for the electric field direction, vari-  
 128 ations in the speed are of minor importance. To ensure that a change in magnetic field  
 129 in the 10 minute interval is not interfering with the electric field estimate, we discard in-  
 130 tervals where more than 20% of the magnetic field vectors deviate by more than  $30^\circ$   
 131 from the mean field vector. These numbers represent a trade-off between retaining clear in-  
 132 tervals and larger statistics. Note that changing them does not alter the results qual-  
 133 itatively.

134 We also use the CSEQ (cometocentric solar equatorial) system, where the x-axis  
 135 points towards the Sun, the z-axis is aligned with the solar North pole and the y-axis  
 136 completes the right handed system. The gas production rate is derived using the in-situ  
 137 data from ROSINA-COPS (Balsiger et al., 2007) and a spherical coma model (Haser,  
 138 1957).

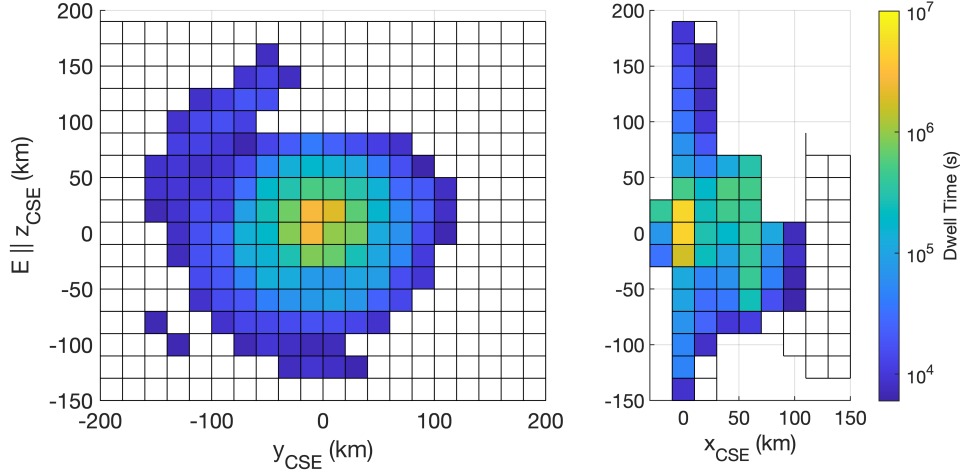


**Figure 2.** Spacecraft dwell time in the same coordinate system as Fig. 1. Note that the colour scale is logarithmic. White patches indicate that the dwell time is below the cut-off of 6000 s.

139

### 3 Results and Discussion

140

#### 3.1 Location of the Wave Detections

141

142

143

144

145

146

147

148

149

150

151

The locations in the CSE frame at which waves are detected are shown in Fig. 1. The wave occurrence is normalized by the spacecraft dwell times to correct for spatial bias. Grid points with less than 100 minutes dwell time are discarded as the wave determination interval was 10 minutes with a 5 minute overlap and we require at least 20 points for the normalization. Wave occurrence is rather homogenous in the vicinity of the comet, with no specific region dominating. The total occurrence rate of the waves is 0.21% in the  $-E$  hemisphere and 0.28% in the  $+E$  hemisphere. These rates are essentially the same, therefore we conclude that there is no preferred hemisphere for wave detection. We have also performed the same analysis in the CSEQ system with similar results (not shown). This does not agree with the simulations by Koenders et al. (2016), where the waves were only seen in the  $+E$ -hemisphere.

152

153

154

155

156

157

158

159

We present two possible explanations for this discrepancy. First, our findings could indicate that the cross-field current is not part of the generation mechanism. Or second, the coherence length and the source region are much larger than the cometocentric distance that Rosetta covers (150 – 200 km). This means that Rosetta is not able to see any asymmetry with respect to the convective electric field. However, Richter et al. (2016) estimate a coherence length of  $\sim 50$  km and a source region size of up to 100 km, which means that the source region size would be smaller than the covered distance and we therefore should see a difference between the two  $E$  hemispheres.

160

#### 3.2 Wave Power and Frequency Distribution

161

162

163

164

165

166

Fig. 4 shows the time evolution of the frequency as well as the gas production rate and the spacecraft position. The spatial distribution of the wave power was investigated by Richter et al. (2015). We can affirm their finding that the peak PSD increases as the cometocentric distance decreases (see panel 2, 4, 5 of Fig. 4) and that there is no correlation between the PSD and the magnetic field magnitude. This is true for both detection methods.

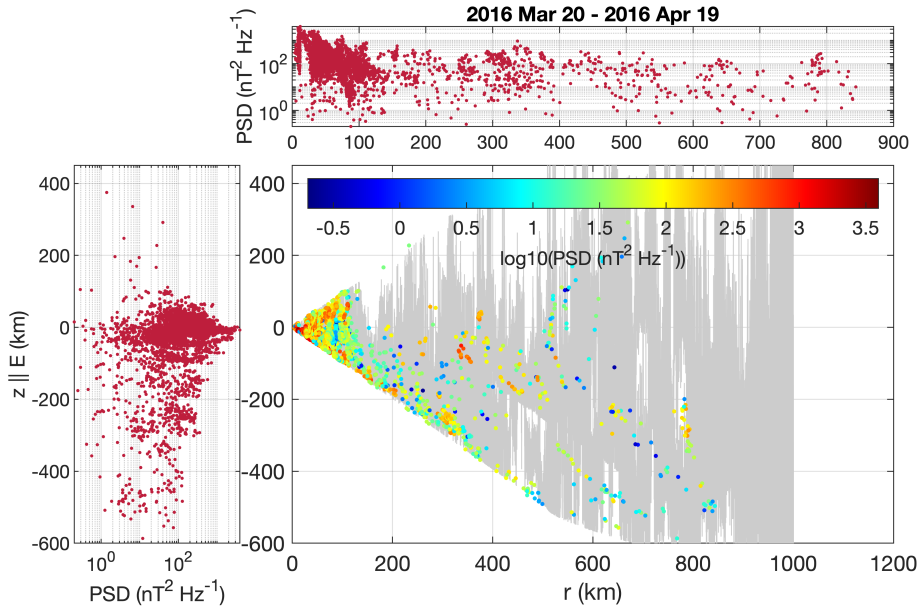


**Figure 3.** Peak wave power spectral density in a cometocentric distance -  $z_{\text{CSE}}$  plot. The power spectral density is color coded and each point corresponds to one 10 minute interval. The grey line follows the position of the spacecraft. The smaller figures to the top and left show the power spectral density over  $r$  and  $z$ .

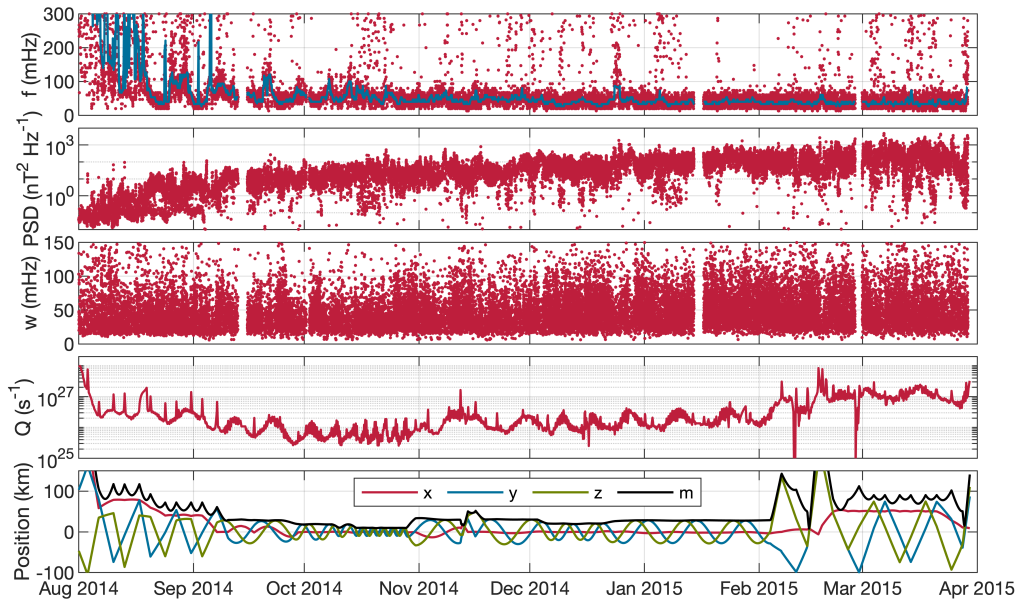


**Figure 4.** From top to bottom: peak frequency (with moving mean in blue), peak power spectral density, width ( $w$ ) of the peak, gas production rate estimate, and spacecraft position in CSEQ. For better visibility, the gas production rate was treated with a moving average over 10000 data points.

167 The frequency does not depend on the cometocentric distance or the magnetic field  
 168 magnitude. The frequency is clearly changing (uppermost panel), from values above 90 mHz  
 169 up until early October to values below 90 mHz afterwards. There is also a distinct os-  
 170 cillating pattern in the higher frequency regime.

171 We have performed a correlation analysis between the frequency and plasma den-  
 172 sity, neutral density, Alfvén velocity, and gas production rate derived from a simple, spher-  
 173 ical model (Haser, 1957) and observations, gas production rate from an empirical model  
 174 (Hansen et al., 2016), spacecraft position in CSEQ, CSE and a comet fixed frame. There  
 175 are no clear correlations found, except that the position of the spacecraft in  $z$  direction  
 176 in CSEQ shows a remarkable similarity. Fig. 5 shows this more clearly. For values of  $z_{\text{CSEQ}}$   
 177 greater than 20 km the frequency increases by a factor of three, compared to other val-  
 178 ues. We have ruled out that this is due to the radial distance, or due to the longitude  
 179 and latitude of Rosetta in the comet-fixed system.

180 Meier et al. (2016) show that the phase structure caused by the ion-Weibel insta-  
 181 bility is highly asymmetric along  $z$  in the CSEQ system (referred to as cometary frame  
 182 of reference in the publication). This is due to the Doppler shift when transforming from  
 183 a current-aligned to a stationary coordinate system. This asymmetry could explain our  
 184 findings here. However, it is unclear why this asymmetry is not visible in the CSE frame  
 185 of reference, as in the theoretical model the  $z$  axis is aligned with the electric field. There  
 186 are also other discrepancies between the model and the findings from the data: for ex-  
 187 ample the model predicts a very steep increase of the frequency with an increase in the  
 188 magnetic field strength. For a magnetic field greater than 15 nT, the frequency is mod-  
 189 eled to be higher than 2 Hz, which is in direct contradiction to the data, where the fre-  
 190 quency overall decreases with higher magnetic fields. However, many parameters change  
 191 at the same time during the Rosetta observation period and thus the interplay of an in-  
 192 crease in solar wind speed, magnetic field pile-up and increase in cometary ion density  
 193 makes it very difficult to disentangle the contributions.

194 Contrary to what Breuillard et al. (2019) find, there is no correlation between the  
 195 frequency and the plasma density. In fact a closer examination of the plasma density and  
 196 frequency reveals intervals where they correlate, intervals where they anti-correlate, and  
 197 intervals where they are  $90^\circ$  out of phase, shedding doubt on the correlation between fre-  
 198 quency and density found by Breuillard et al. (2019). If they were correlated, a period-  
 199 icity in the wave frequency of 6 or 12 hours according to the neutral gas density vari-  
 200 ation (Goetz et al., 2017) should also be visible, which it is not. However, it should be  
 201 noted here that there is still a possibility that the wave frequency is correlated to the  
 202 density in the wave generation region, which as noted above may be much larger than  
 203 the distances covered by the in-situ measurements.

204 For the interval used in this study, Mars was located conveniently close to the Sun-  
 205 comet line. The distance between Mars and the comet was approximately 1.8 AU. At a  
 206 solar wind velocity of 350 km/s to 400 km/s the delay time between Mars solar wind ob-  
 207 servations and solar wind at the comet is around 8 – 9 days. Unfortunately MAVEN  
 208 observations at Mars only start in October 2014, and Mars Express has no magnetic field  
 209 instrument. However, we can compare the Mars Express ASPERA-3 IMA proton mo-  
 210 ments with the observed frequency development. There is no obvious correlation, espe-  
 211 cially considering the uncertainty in the solar wind propagation. Earth was in a disad-  
 212 vantageous position compared to the comet, so propagation models are not optimal. No  
 213 obvious correlation can be found with solar wind parameters propagated from Earth (Tao  
 214 et al., 2005).

215 The width of the peak also does not correlate clearly with any of the investigated  
 216 parameters. One could, maybe infer from Fig. 4 that the width slightly increases with  
 217 gas production rate. One possible explanation could be that the density in the wave gen-  
 218 eration region, or the size of the wave generation region itself modify the frequency and

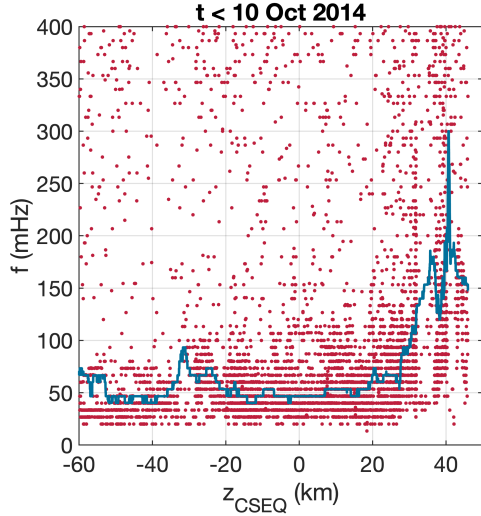


**Figure 5.** Frequency of the wave over the  $z$ -coordinate in the CSEQ system. The blue line shows a moving average.

219 during the higher activity times waves are generated at more frequencies increasing the  
 220 width of the peak.

## 221 4 Conclusions

222 We have performed a study of the properties of low-frequency waves in the plasma  
 223 environment of comet 67P. A new method allows for the distinction of intervals where  
 224 the waves are present and intervals where they are not observable. We find that:

- 225 • waves occur everywhere in the cometary environment, regardless of electric field  
 226 direction.
- 227 • the wave generation region can tentatively be constrained to  $> 800$  km.
- 228 • the wave frequency changes from  $> 90$  mHz at large heliocentric distances to  $<$   
 229  $90$  mHz at smaller heliocentric distances.
- 230 • the wave frequency is not a function of the plasma density.
- 231 • the wave frequency during the earliest stages of cometary activity depends on the  
 232 spacecraft position in CSEQ.
- 233 • the wave width changes from low at large heliocentric distances to high at small  
 234 heliocentric distances.

235 Thus we found that the wave generation region is larger than previously estimated and  
 236 that the in-situ plasma density is not the driver of the wave frequency. To constrain this  
 237 further measurements with two spacecraft and/or more statistics are necessary.

238 The findings are partly in agreement with the predictions for a modified ion-Weibel  
 239 instability, however they disagree with the hybrid simulations which predicted an asym-  
 240 metry in the wave occurrence along the convective electric field direction.

## 241 Acknowledgments

242 Datasets of the RPC-MAG, RPC-LAP and ROSINA instruments onboard Rosetta as  
 243 well as the dataset of the ASPERA-3 instrument onboard Mars Express are available

244 at the ESA Planetary Science Archive (Besse et al., 2018, <http://archives.esac.esa.int/psa>).  
 245 CG is supported by an ESA Research Fellowship.

## 246 References

- 247 Balsiger, H., Altwegg, K., Bochsler, P., Eberhardt, P., Fischer, J., Graf, S., . . .  
 248 Wollnik, H. (2007, February). Rosina Rosetta Orbiter Spectrometer for  
 249 Ion and Neutral Analysis. *Space Science Reviews*, *128*, 745–801. doi:  
 250 10.1007/s11214-006-8335-3
- 251 Behar, E., Nilsson, H., Wieser, G. S., Nemeth, Z., Broiles, T. W., & Richter,  
 252 I. (2016, February). Mass loading at 67P/Churyumov-Gerasimenko: A  
 253 case study. *Geophysical Research Letters*, *43*, 1411–1418. doi: 10.1002/  
 254 2015GL067436
- 255 Besse, S., Vallat, C., Barthelemy, M., Coia, D., Costa, M., De Marchi, G., . . .  
 256 Vallejo, F. (2018, Jan). ESA’s Planetary Science Archive: Preserve and present  
 257 reliable scientific data sets. *Planetary and Space Science*, *150*, 131-140. doi:  
 258 10.1016/j.pss.2017.07.013
- 259 Breuillard, H., Henri, P., Bucciantini, L., Volwerk, M., Karlsson, T., Eriksson, A.,  
 260 . . . Hajra, R. (2019). The properties of the singing comet waves in the  
 261 67P/Churyumov-Gerasimenko plasma environment as observed by the Rosetta  
 262 mission. *Astron. Astrophys.* doi: 10.1051/0004-6361/201834876
- 263 Edberg, N. J. T., Eriksson, A. I., Vigren, E., Johansson, F. L., Goetz, C., Nilsson,  
 264 H., . . . Henri, P. (2019, jul). The convective electric field influence on the  
 265 cold plasma and diamagnetic cavity of comet 67p. *The Astronomical Jour-*  
 266 *nal*, *158*(2), 71. Retrieved from [https://doi.org/10.3847/1538-3881/](https://doi.org/10.3847/1538-3881/2F1538-3881/2Fab2d28)  
 267 [2F1538-3881/](https://doi.org/10.3847/1538-3881/ab2d28)  
 268 [2Fab2d28](https://doi.org/10.3847/1538-3881/ab2d28) doi: 10.3847/1538-3881/ab2d28
- 269 Glassmeier, K.-H. (2017, July). Interaction of the solar wind with comets: A rosetta  
 270 perspective. *Philosophical Transactions of the Royal Astronomical Society A*,  
 271 *375*, 20160256. doi: 10.1098/rsta.2016.0256
- 272 Glassmeier, K.-H., Boehnhardt, H., Koschny, D., Kührt, E., & Richter, I. (2007,  
 273 February). The Rosetta Mission: Flying Towards the Origin of the Solar  
 274 System. *Space Science Reviews*, *128*, 1–21. doi: 10.1007/s11214-006-9140-8
- 275 Glassmeier, K.-H., Richter, I., Diedrich, A., Musmann, G., Auster, U., Motschmann,  
 276 U., . . . Tsurutani, B. (2007, February). RPC-MAG The Fluxgate Magne-  
 277 tometer in the ROSETTA Plasma Consortium. *Space Science Reviews*, *128*,  
 278 649–670. doi: 10.1007/s11214-006-9114-x
- 279 Goetz, C., Volwerk, M., Richter, I., & Glassmeier, K.-H. (2017, July). Evolution  
 280 of the magnetic field at comet 67P/Churyumov-Gerasimenko. *Monthly No-*  
 281 *tices of the Royal Astronomical Society*, *469*, S268–S275. doi: 10.1093/mnras/  
 282 stx1570
- 283 Grün, E., Agarwal, J., Altobelli, N., Altwegg, K., Bentley, M. S., Biver, N., . . .  
 284 Taylor, M. G. G. T. (2016, November). The 2016 Feb 19 outburst of comet  
 285 67P/CG: an ESA Rosetta multi- instrument study. *Monthly Notices of the*  
 286 *Royal Astronomical Society*, *462*, S220–S234. doi: 10.1093/mnras/stw2088
- 287 Hajra, R., Henri, P., Vallières, X., Galand, M., Héritier, K., Eriksson, A. I., . . . Ru-  
 288 bin, M. (2017, November). Impact of a cometary outburst on its ionosphere.  
 289 Rosetta Plasma Consortium observations of the outburst exhibited by comet  
 290 67P /Churyumov-Gerasimenko on 19 February 2016. *Astron. Astrophys.*, *607*,  
 291 A34. doi: 10.1051/0004-6361/201730591
- 292 Hansen, K. C., Altwegg, K., Berthelier, J.-J., Bieler, A., Biver, N., Bockelée-Morvan,  
 293 D., . . . Rosina Team (2016, September). Evolution of water production of  
 294 67P/Churyumov-Gerasimenko: An empirical model and a multi-instrument  
 295 study. *Monthly Notices of the Royal Astronomical Society*, *462*, S491–S506.  
 296 doi: 10.1093/mnras/stw2413

- 296 Haser, L. (1957). Distribution d'intensité dans la tête d'une comète. *Bulletin de la*  
 297 *Societe Royale des Sciences de Liege*, 43, 740–750.
- 298 Heinisch, P., Auster, H. U., Richter, I., Haerendel, G., Apathy, I., Fornacon, K. H.,  
 299 ... Glassmeier, K. H. (2017, Jul). Joint two-point observations of LF-waves  
 300 at 67P/Churyumov—Gerasimenko. *Mon. Not. R. Astron. Soc.*, 469, S68-S72.  
 301 doi: 10.1093/mnras/stx1175
- 302 Koenders, C., Perschke, C., Goetz, C., Richter, I., Motschmann, U., & Glassmeier,  
 303 K. H. (2016, October). Low-frequency waves at comet 67P/Churyumov-  
 304 Gerasimenko. Observations compared to numerical simulations. *Astron. Astro-*  
 305 *phys.*, 594, A66. doi: 10.1051/0004-6361/201628803
- 306 Meier, P., Glassmeier, K.-H., & Motschmann, U. (2016, Aug). Modified ion-Weibel  
 307 instability as a possible source of wave activity at Comet 67P/Churyumov-  
 308 Gerasimenko. *Ann. Geophys.*, 34(9), 691-707. doi: 10.5194/angeo-34-691-2016
- 309 Richter, I., Auster, H.-U., Berghofer, G., Carr, C., Cupido, E., Fornacon, K.-H.,  
 310 ... Glassmeier, K.-H. (2016, July). Two-point observations of low-frequency  
 311 waves at 67P/Churyumov-Gerasimenko during the descent of PHILAE: com-  
 312 parison of RPCMAG and ROMAP. *Annales Geophysicae*, 34, 609–622. doi:  
 313 10.5194/angeo-34-609-2016
- 314 Richter, I., Koenders, C., Auster, H.-U., Frühauff, D., Götz, C., Heinisch, P., ...  
 315 Glassmeier, K.-H. (2015, August). Observation of a new type of low-frequency  
 316 waves at comet 67P/Churyumov-Gerasimenko. *Annales Geophysicae*, 33,  
 317 1031–1036. doi: 10.5194/angeo-33-1031-2015
- 318 Tao, C., Kataoka, R., Fukunishi, H., Takahashi, Y., & Yokoyama, T. (2005, Novem-  
 319 ber). Magnetic field variations in the Jovian magnetotail induced by solar  
 320 wind dynamic pressure enhancements. *Journal of Geophysical Research (Space*  
 321 *Physics)*, 110(9), 11208. doi: 10.1029/2004JA010959
- 322 Volwerk, M., Goetz, C., Richter, I., Delva, M., Ostaszewski, K., Schwingenschuh,  
 323 K., & Glassmeier, K.-H. (2018). A tail like no other: RPC-MAG's view of  
 324 Rosetta's tail excursion at comet 67P/Churyumov-Gerasimenko. *Astron.*  
 325 *Astrophys.*, 614, A10. doi: 10.1051/0004-6361/201732198